Study on the Anodic Oxide Films formed on Mg Alloys Using DC, AC Methods in Alkaline Solution

S. A. Salman

Abstract— Magnesium is the lightest of all structural metal materials in practical use, with a density equivalent to two-thirds that of Al, one-third that of Zn and one quarter that of steel. However, applications of wrought Mg alloys have not been as successful as those of aluminum (Al) alloys because of the high corrosion susceptibility under certain service conditions. In this research, we have investigated the DC/AC anodizing of AZ31 Mg alloy samples in alkaline NaOH solutions under various applied potentials. In the DC anodizing experiments, the current density showed a maximum value at a potential of 3 V, and thicker anodic films were obtained at this potential. The films formed at lower potentials were mainly composed of magnesium hydroxide, and the films formed at higher potentials were composed of magnesium hydroxide and magnesium oxide. At AC anodizing experiments, the anodic coatings formed at 10 V AC potential had the best anticorrosion resistance compared with the other anodic coatings. At DC anodizing, thicker anodic films with a high corrosion resistance were obtained at a potential of 3 V. However, a potential of ±10 V showed better corrosion resistance for AC anodizing.

Index Terms— Anodizing, Pulse, Magnesium, Alkaline, Corrosion, Alkaline, Coating.

◆

1 INTRODUCTION

Magnesium is the lightest applied structural metal; it has many other desired properties, such as a high specific strength and good electromagnetic shielding. Furthermore, some magnesium alloys are well known as damping materials. Therefore, magnesium alloys are very attractive for many applications, especially when a reduction in weight is needed. Magnesium alloys are widely used in structural and industrial materials, such as in aerospace equipment, in automobiles, in electronic sporting goods, and in handheld tools.

Poor corrosion resistance is a major problem that limits the widespread use of magnesium alloys. Therefore, surface treatments are applied to protect magnesium alloys against corrosion and to improve their surface properties. There are many methods that have been applied as surface treatments, such as electroplating, plasma spraying, chemical vapor deposition, anodizing, and conversion coating [1-4]. Anodizing in hexavalent chromium-containing solutions has been commonly applied over the last decade. However, because of the toxicity of these solutions and because of environmental and recycling problems, there has been a push to replace chromates that contain hexavalent chromium ions. Anodizing and conversion coatings are carried out in environment friendly solutions, such as alkaline-, cerium-, vanadate- and phosphate-based solutions [5–10].

Recently, intensive research has been carried out to develop the anodizing process in alkaline solutions containing various additives, such as borate, aluminate, and silicate ions [11, 12].
In another development in this process, some studies have explored the idea of using either a pulsed current or potential (pulse anodizing) instead of a constant applied source to obtain a higher mean current density and thereby to decrease the processing time and total energy consumption [13]. Zn–Ni alloy coatings were plated on AZ91 magnesium alloy using a pulse potential electrodeposition method. The pulse current electrodeposition process can bring about homogeneous and compact Zn–Ni coatings with good corrosion resistance [14].

In our previous research, we examined the effect of square pulse anodizing on the surface morphology and corrosion characteristics of AZ31 Mg alloy samples for different duty ratios between the transpassive (10 V Ag/AgCl) and active regions (1.35 V Ag/AgCl). The corrosion resistance was improved and the surface porosity was decreased by approximately 11 times compared with samples obtained using a constant potential [15]
In this research, we have investigated the anodizing of AZ31 Mg alloy samples in alkaline NaOH solutions under DC and AC voltages. The polarization behavior and the effect of the applied potential were investigated.

2 EXPERIMENTAL METHODS

The chemical composition of the AZ31 Mg alloy used is shown in Table 1.

Table 1 Chemical composition (mass %) of AZ31 Mg alloy

Element	Mg	Al	Zn	Mn	Si	Cu	Ni	Fe
Conc.	Bal.	3.0	1.0	0.43	0.01	<0.01	<0.001	0.003

The samples were first abraded using emery paper up to 2000 grit, polished with alumina powder (diameter = 0.05 μm), washed using deionized water, and then dried in cool air using a handheld dryer.
The samples were subjected to a treatment in 200 ml of a 1 M

- *S.A. Salman is working at Faculty of Engineering, Al-Azhar University, Nasr City, Cairo, Egypt and currently Pursuing postdoctoral fellowship in School of Engineering, Nagoya University, Nagoya, Japan*
- *E-mail: sa.salman@yahoo.com*

NaOH solution at 298 K under AC and DC voltages for 600 s. The anodizing was performed at various p–p voltages changing from 0 to 50 V. The frequency was set to 1 Hz in the AC method.

The surface and cross-sectional microstructures and corresponding chemical composition of the samples were characterized using scanning electron microscopy (SEM) and X-ray diffraction (XRD). The corrosion resistance was examined using the potentiodynamic polarization method. The polarization tests were carried out using a Solartron 1285 potentiostat employing a scan rate of 1 mV/s in a 17 mM NaCl and 0.1 M Na2SO4 solution at 298 K in a three-electrode cell with the coated samples as the working electrode, an Ag/AgCl/sat KCl as the reference electrode, and a platinum coil as the counter electrode. The potential difference, ΔE, was used to compare the pitting potential results. ΔE was defined as the difference between the anodic potential values at 1 mAcm2 for both anodized and nontreated samples.

3 RESULTS AND DISCUSSION

3.1 Polarization measurements using a DC method

The polarization measurements of AZ31 Mg alloy samples using a DC method were carried out in 200 ml of an alkaline 1 M NaOH solution at pH = 13.5 and 298 K. The starting potential was set to 0 V moving toward the anode direction using a scanning rate of 0.1 Vs^{-1}. Figure 1 shows that while the cathode current flowed, an accompanying intense gas evolution on the surface of the sample occurred at a potential of ≤ 0 V, and an overcurrent occurred near the potential of –5 V. Hydrogen was liberated from the decomposition of water according to the following equation.

Figure 1

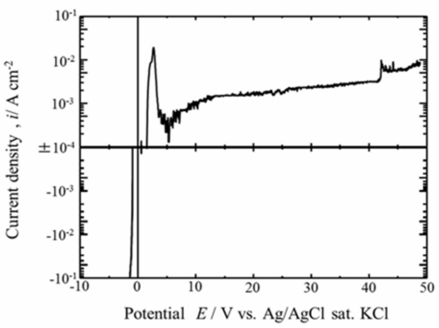

Fig. 1. Polarization curve of AZ31 in 1 M NaOH solution of 298 K using DC voltage at scanning speed of 0.1V s^{-1} .

$$2H_2O + 2e^- \rightarrow H_2 + 2OH^-$$

On the other hand, on the anode side, the current density showed a maximum value at a potential of 3 V. During this process, magnesium dissolution occurred, and an intensive generation of oxygen gas was observed. The color of the solution turned to a light gray because of the active movement of the liberated gases. The current density then decreased again because of the formation of a layer of magnesium hydroxide on the sample. The following equations explain the active dissolution and passivation reactions of magnesium and the gas evolution process.

$$Mg \rightarrow Mg^{2+} + 2e^- \qquad (1)$$

$$Mg^{2+} + 2OH^- \rightarrow Mg\,(OH)_2 \qquad (2)$$

$$Mg\,(OH)_2 \rightarrow Mg^{2+} + \tfrac{1}{2}\,O_2 + H_2O + 2e^- \qquad (3)$$

$$4OH^- \rightarrow O_2 + 2H_2O + 4e^- \qquad (4)$$

At a potential starting from 10 to 50 V, only a slight liberation of gas occurred, and a lower current flow was observed. A possible reason for this is the formation of a passive MgO layer. Magnesium oxide can form according to equation (5). Several reports have demonstrated that the above compounds can be interconverted between each other by either hydration or dehydration processes [1, 17].

$$Mg(OH)_2 \rightarrow MgO + H_2O \qquad (5)$$

3.2 Polarization measurements using an AC method

The polarization measurements using an AC method were carried out in 200 ml of a 1 M alkaline NaOH solution at pH = 13.5 and 298 K. An alternating current was applied as a sine wave with a frequency of 1 Hz. The maximum positive value of E (E_T) was set to be equal to the negative minimum value of –E (–E_B). The polarization was measured using a scan rate of 0.1 Vs–1 up to E_T.

Figure 2-a shows the potential and current density of a single cycle, single cycle run, where i_1 represents the anode maximum current value in the forward path, i_2 represents the current value at the maximum potential of the first half of the cycle, and i_3 represents the maximum current value in the second half of the cycle.

Fig.2-b shows the polarization for 30 s; almost no current flowed at 0 V, but the current density began to increase from 6 V, reaching its highest value at 9 V: this potential represents the active region. Subsequently, the current density decreased up to 12 V, and then increased again at a stable rate. Among these three current regions, the highest gradient with a sharp increase in the current density was located at i_1 and i_3 between 10 and 20 V. This could refer to a second active region. The current density increased at a stable rate on further increasing the potential, but i_1 increased at a faster rate than i_3 did. This may be from the formation of MgO, which would lead to a decrease in the potential.

In the case of i_2, the voltage did not change for most of the scanning speeds because i_2 represents the value of the current at the maximum potential of the first half of the cycle.

Therefore, an increase in i_2 is considered to have a greater impact than changes in the voltage scan rate because it involves an increase in the value of ET. The increase in gradient between 20 and 50 V of i2 is similar to that observed for i1.

Figure 2

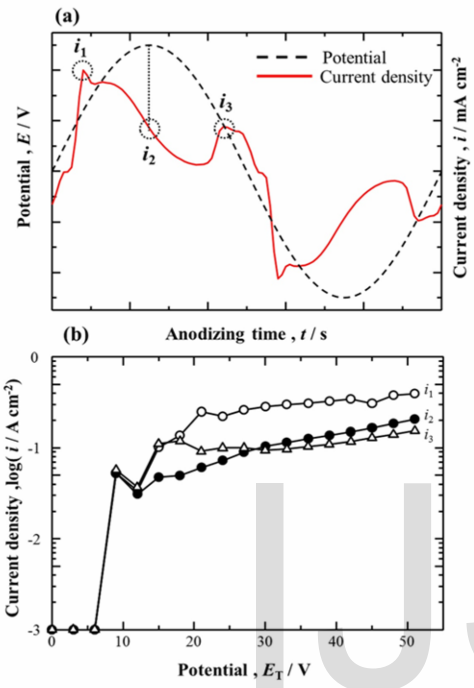

Fig. 2. Polarization curve of AZ31 in 1 M NaOH solution of 298 K using AC voltage at scanning speed of 0.1V s-1 . (a) One cycle polarization and (b) 30 s polarization.

3.2 Effect of changes in potential

The anodizing process was carried out in 200 ml of a 1 M NaOH solution at 298 K and pH = 13.5 for 600 s. The value of ET was set to be equal to the value of –EB. Anodic films were obtained at 7.5, 10, 20, 30, 40, and 50 V. The films formed at a potential of (7.5 V, –7.5 V) and (10 V, –10 V) had a uniform skin-colored film. The surface between a potential of 20 and 50 V was uniformly white. The mirrored surface of the substrate was still visible after anodizing at (30 V, –30 V), which indicates the formation of a very thin film.
The SEM images shown in Fig. 3 show the surface morphologies of the anodic films. At a potential of (7.5 V, –7.5 V), the anodic films had a porous structure, and those formed at (10 V, –10 V) contained some visible cracks. On the other hand, the films formed at higher potentials had irregular, rough surfaces with a flake-like structure.

Figure 3

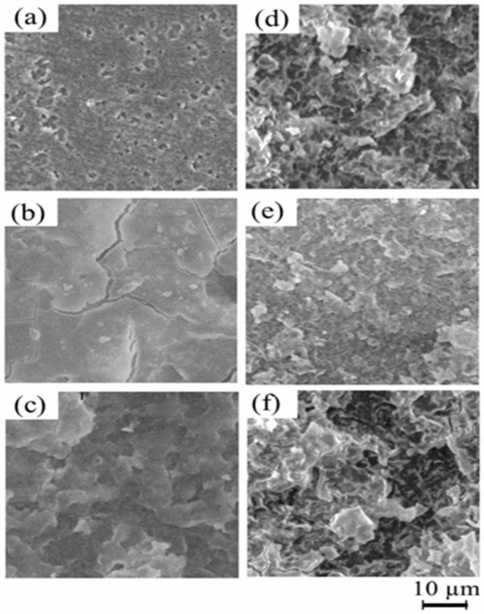

Fig. 3. Surface SEM images of the anodic film obtained by AC anodizing in sine wave of 1Hz and applied potential of (a)7.5 V, (b)10 V, (c)20 V, (d)30 V, (e)40 V and (f)50 V

Figure 4 shows the relationship between the film thickness and the applied voltage. The film thickness increased with increasing potential and reached a maximum film thickness of 3 μm at a potential of 10 V. The film thickness then decreased to its lowest thickness of 0.3 μm at 30 V. On increasing the potential above 30 V, the thickness of the film increased again to 1.0 μm at 50 V.

The volume fraction analysis of AZ31 Mg alloy from XRD data before and after anodizing at various potentials is shown in

Figure 4

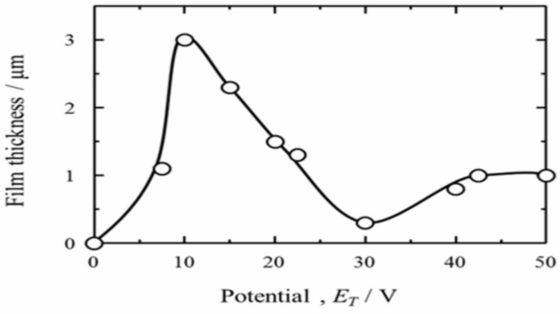

Fig. 4. The relation between the film thickness and the voltage of the film produced in a sine wave of 1Hz

Fig. 5. The anodic films produced at a potential of 10 V were

mainly composed of $Mg(OH)_2$, while the anodic films produced at a potential of 50 V contained $Mg(OH)_2$, and MgO had formed on the film. This explains the thicker coating obtained at lower voltages, as the samples contained a large amount of $Mg(OH)_2$. On the other hand, a thinner coating was obtained at higher potentials because the film changed from $Mg(OH)_2$ to MgO and consequently decreased in volume.

Figure 5

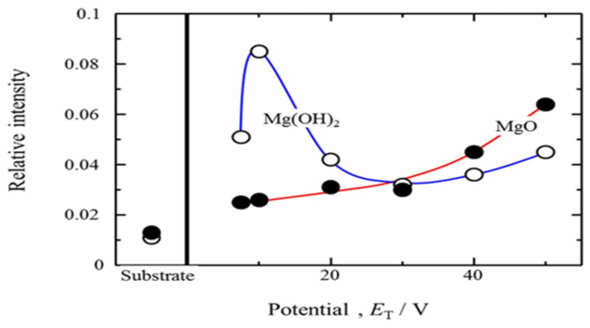

Fig. 5. The relation between the film thickness and the voltage of the film produced in a sine wave of 1Hz

Figure 6

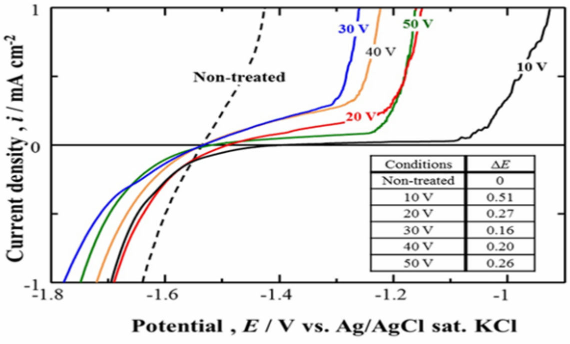

Fig. 6. Polarization curves of AZ31 Mg alloy samples before and after anodizing under various applied AC potentials

The potentiodynamic polarization method was used to characterize the corrosion properties of the AZ31 Mg alloy samples before and after the anodizing treatment. Figure 6 shows the anodic and cathodic polarization curves of AZ31 Mg alloy samples before and after anodizing under various applied AC potentials. All the anodized samples had a less negative pitting potential, which means that the anodizing treatment improved the corrosion resistance. However, the coatings obtained at a potential of 10 V had the most notable pitting potential and the highest value of ΔE. On the other hand, the coatings obtained at a potential of 30 V had the lowest pitting potential and consequently exhibited a poor corrosion resistance compared with the other anodic coatings. These results show that the thickness of the films played an important role in the enhancement of the corrosion resistance as shown in Fig. 6.

CONCLUSION

In the DC anodizing experiments, the current density showed a maximum value at a potential of 3 V, and thicker anodic films were obtained at this potential. The films formed at lower potentials were mainly composed of magnesium hydroxide, and the films formed at higher potentials were composed of magnesium hydroxide and magnesium oxide.

In the AC anodizing experiments, the film thickness increased with increasing potential and reached a maximum film thickness of 3 µm at a potential of 10 V. The film thickness then decreased to 0.3 µm at a potential of 30 V.

The anodic coatings formed at 10 V AC potential had the best anticorrosion resistance compared with the other anodic coatings.

ACKNOWLEDGEMENT

The author gratefully acknowledge the financial support of Aichi Center for Industry and Science Technology and the Ministry of the Education, Culture, Sports, Science and Technology, Japan. and the Ministry of Higher Education, Egypt

REFERENCES

[1] S. A. Salman, M. Okido, Anodization of magnesium (Mg) alloys to improve corrosion resistance, in: G-L Song (Eds.), Corrosion prevention of magnesium alloys, Woodhead Publishing, Cambridge, 2013, pp. 197-231.

[2] S.A. Salman, M.Okido, Self-assembled monolayers formed on AZ31 Mg alloy, Journal of Physics and Chemistry of Solids, 73 (2012) 863.

[3] T.F. da Conceicao, N. Scharnagl, C. Blawert, W. Dietzel, K.U. Kainer, Surface modification of magnesium alloy AZ31 by hydrofluoric acid treatment and its effect on the corrosion behaviour, Thin Solid Films, 518 (2010) 5209-5218.

[4] Long-Hao Li, T.S.N. Sankara Narayanan, Yu Kyoung Kim, Young-Min Kong, Il Song Park, Tae Sung Bae, Min Ho Lee, Deposition of microarc oxidation–polycaprolactone duplex coating to improve the corrosion resistance of magnesium for biodegradable implants, Thin Solid Films, 562 (2014) 561-567.

[5] S. A. Salman, Ryoichi Ichino, and Masazumi Okido, Development of Cerium-based Conversion Coating on ZA31 Magnesium Alloy, Chem. Lett. 36 (2007) 1024.

[6] S. A. Salman, R. Ichino and M. Okido, Production of Alumina-Rich Surface Film on AZ31 Magnesium Alloy by Anodizing with Co Precipitation of Nano-Sized Alumina, Mater. Trans. 49 (2008) 1038.

[7] Y. Mizutani, S.J. Kim, R. Ichino, M. Okido, Anodizing of Mg alloys in

alkaline solutions, Surface and Coatings Technology, 169–170 (2003) 143-146.

[8] S. A. Salman, R. Ichino and M. Okido, Influence of calcium hydroxide and anodic solution temperature on corrosion property of anodising coatings formed on AZ31 Mg alloysSurface Engineering 24 (2008) 242.

[9] S. A. Salman, R. Ichino and M. Okido, Improvement of corrosion resistance of AZ31 Mg alloy by anodizing with co-precipitation of cerium oxide, Trans. Nonferrous Met. Soc. China, 19 (2009) 883.

[10] Salman, S. A., Kuroda, K. and Okido, M. (2013) Formation of Vanadate Conversion Coating on AZ31 Magnesium Alloy, in Magnesium Technology 2013 (eds N. Hort, S. N. Mathaudhu, N. R. Neelamegghham and M. Alderman), John Wiley & Sons, Inc., Hoboken, NJ, USA. doi: 10.1002/9781118663004.ch30.

[11] .S. Jang, Y.K. Kim, I.S. Park, S.J. Lee, M.H. Lee, J.M. Yoon, T.S. Bae, Film characteristics of anodic oxidized AZ91D magnesium alloy by applied power, Surf. Interface Anal. 41 (2009) 524–530.

[12] L. Chai, X. Yu, Z. Yang, Y. Wang, M. Okido, Anodizing of magnesium alloy AZ31 in alkaline solutions with silicate under continuous sparking, Corros. Sci. 50 (2008) 3274–3279.

[13] A.D. Juhl, Pulse anodizing of extruded, cast aluminium alloys, Ph.D. thesis, Inst.of Manufacturing Engineering, The Technical University of Denmark (1999).

[14] Y.F. Jiang, L.F. Liu, C.Q. Zhai, Y.P. Zhu, W.J. Ding, Corrosion behavior of pulse-plated Zn–Ni alloy coatings on AZ91 magnesium alloy in alkaline solutions, Thin Solid Films, 484 (2005) 232-237.

[15] YI Choi, S Salman, K Kuroda, M Okido, Improvement in corrosion characteristics of AZ31 Mg alloy by square pulse anodizing between transpassive and active regions, Corrosion Science 63 (2012) 5-11.

[16] G. Song and Atrens, A. Proceedings of the 6th International Conference Magnesium Alloys and Their Applications, Wiley-VCH, Weinheim, p. 507, 2004.

[17] M. Laska, J. Valtyni and P. Feller, Crystal Research and Technology, Influence of pH on the Crystal Size Distribution of Mg(OH)2 Prepared by the Hydration of MgO, 28 (1993) 931.